DOI: 10.13208/j.electrochem.131174 **Artical ID**:1006-3471(2014)05-0416-10
Cite this: *J. Electrochem.* **2014**, *20*(5): 416-425 **Http**://electrochem.xmu.edu.cn

Influence of Pt:Ru Ratio in Nanotubes Array Structures on the Electrocatalytic Activity of Methanol Oxidation

YUAN Jin-hua, WANG Feng-bin, XIA Xing-hua*
(*State Key Laboratory of Analytical Chemistry for Life Science, School of Chemistry and Chemical Engineering, Nanjing University, Nanjing* 210093, *China*)

Abstract: Bimetallic PtRu nanotubes array electrodes (NTAEs) with varied Pt to Ru atomic ratios have been prepared by electrochemical codeposition in 3-aminopropyltri-methoxysilane modified porous anodic alumina (PAA) membranes. The structure and morphology of the catalysts were characterized using X-ray diffraction (XRD) and scanning electron microscopy (SEM), respectively. Electrochemical results showed that the NTAEs with varied atomic ratios could be achieved by controlling the precursor concentration for deposition. The prepared nanoarrays composed of Pt or PtRu alloy promoted the mass-normalized activity toward the sluggish electrooxidation reaction of methanol due to the increased catalytic activity and real surface area, as well as the improved mass transport through the catalysts. Correlations between the anode composition and the electrocatalytic activity of the catalysts toward the electrooxidations of CO and CH_3OH were systemically investigated. The PtRu NTAEs containing ca. 50% Ru showed the highest activity for CO electrooxidation, while the PtRu NATEs of 40% Ru for CH_3OH electrooxidation.

Key words: electrocatalysts; PtRu; nanotubes; methanol; CO
CLC Number: TM911.46 **Document Code**: A

Direct methanol fuel cells (DMFCs) have been attracting widespread attentions due to their promising applications as low-temperature compact power-sources[1]. Platinum (Pt) is a good catalyst for the electrooxidation of methanol. However, Pt catalyst is susceptible to the poisoning of CO and other strongly adsorbed intermediates, its practical application as an anode in DMFC is limited[2-3]. Therefore, CO tolerant multi-metallic alloy catalysts such as PtRu[4-6], PtSn[7-8], PtPb[9-10], PtRuRh[11], PtRuOs[12] have been proposed. Among these alloying catalysts, PtRu alloy is the mostly studied system due to its superior activity toward the electrooxidation of methanol. Bifunctional mechanism and ligand effect are usually considered to explain the promoting electrocatalytic activity of the PtRu catalysts. In the bifunctional mechanism, CO-like poisoning intermediates formed from the decomposition of methanol on Pt sites are subsequently oxidized to CO_2 by the surface oxygenated species on the neighbouring Ru sites at lower overpotential[13-17]. In the latter case, the Ru atoms in the alloy induce changes in the electronic configuration of the Pt atoms, which accelerates the direct oxidation of methanol. No matter which mechanism functions, it is clear that the practical performance of the PtRu catalysts strongly depends on the surface compositions of Pt and Ru. In addition, the morphology would affect the catalytic activity of the catalysts. For

Received: 2014-02-13, Revised: 2014-05-14 *Corresponding author, Tel: (86-25)83597436, E-mail: xhxia@nju.edu.cn
This work was financially supported by the National 973 Basic Research Program (No. 2012CB933800), the National Natural Science Foundation of China (No. 21035002, No. 21275070, No. 21205059), the National Science Fund for Creative Research Groups (No. 21121091) and Nanjing Medical Science and Technique Development Foundation(No. QRX11129)

this propose, mesoporous/single crystalline Pt [18] and Pt/Ru[19], Pt/Ru nanowire network[20], Pt/Ru[21]and Pt/Sn[22] nanotubes have been synthesized. Enhanced electrocatalytic activities of these mesoporous materials were observed due to the improved mass transport of fuels and catalytic activities of the mesoporous structures[23-24].

Template-directed synthesis based on PAA membranes was pioneered by Martin's group [25-26]. Using this technique, desired nanotubes and nanowires have been successfully synthesized [27-28]. The PAA template with size-controlled and diameter-uniformed cylindrical pores has been attracting considerable attention for its simple fabrication and inexpensive technology[29-30]. With the help of appropriate molecular anchors modifying the pore wall, highly ordered nanotubes arrays could be successfully prepared[25, 27, 31-32].

Herein, we reported the preparation of highly ordered nanotubes arrays of Pt and PtRu alloys with varied atomic ratios of Pt to Ru using the template synthesis technique and electrochemical codeposition method. The prepared nanotubes arrays were characterized by XRD and SEM. The catalytic activity of the nanotubes arrays with various atomic ratios of Pt to Ru toward the electrooxidations of CO and CH_3OH were systematically studied.

1 Experimental

1.1 Reagents and Instruments

PAA templates were obtained from Whatman International Ltd. (Maidstone, England). CO gas with 0.9999 purity was obtained from Nanjing Weichuang Gas Ltd. Co.. Methanol, 3-aminopropyltrimethoxysilane, sulfuric acid, potassium chloroplatinate, and ruthenium chloride were of analytical grade. Solutions were prepared with distilled water from pure system (>18.2 MΩ·cm, PureLab Classic Co., USA).

All electrochemical experiments were carried out on a CHI 1140 electrochemical workstation (CH Instrument Co., USA). Traditional three-electrode system involving a counter electrode of Pt net, a working electrode of Pt/Ru nanotubes array layer supported on gold substrates (ϕ= 4 mm, geometric area of 0.13 cm^2 was accessible to solution) and a saturated calomel electrode (SCE) or a reversible hydrogen electrode (RHE) were employed. The SCE and RHE were used, respectively, for electrodeposition of nanotubes array and electrochemical characterization of the NTAEs. The current density was reported as the ratio of the current to the real surface area which will be described in the section of results.

The PtRu NTAEs were characterized with a scanning electron microscope (Hitachi SEM-X650, Japan) at an acceleration voltage of 20 kV. Detailed morphologies of all samples and electric diffraction (ED) pattern of the NTAEs were measured on a JEM-200CX TEM (JEM-100s JEOL, Japan). HRTEM analysis was carried out on a JEM-2010 instrument (JEOL, Japan) at an acceleration voltage of 200 kV. X-ray diffraction measurements were performed on an X'Pert Pr X-ray diffraction (X'TRA, Swiss, ARL Co.). The molar ratios of Pt to Ru of the electrodeposited electrodes were measured by EDAX (Energy Dispersing Analysis of X-rays) (PV9100, USA, EDAX Co.).

1.2 Codeposition Procedure

To synthesize nanotubes arrays of PtRu bimetallic catalysts, the pore wall of porous anodic alumina membrane was first silanized by immersing it in a 1% (*V*/*V*) solution of 3-aminopropyltrimethoxysilane for 30 min. Then, the template was rinsed ultrasonically with distilled water for three times. Finally, a thin layer of Au film was evaporated on one side of the silanized membranes as connector to the working electrode port of the potentiostat via a gold disk and copper wire.

The Pt NTAE was electrochemically deposited at -0.1 V (vs. SCE) from a solution of 0.077 mol·L^{-1} H_2PtCl_6 + 0.5 mol·L^{-1} H_2SO_4. PtRu NTAEs with different molar ratios were electrochemically codeposited at -0.1 V from solutions of 0.077 mol·L^{-1} H_2PtCl_6 + 0.077*x* mol·L^{-1} $RuCl_3$ (*x* = 0.3, 0.5, 1, 2, 3) + 0.5 mol·L^{-1} H_2SO_4.

Deposition charge of 9.6 C·cm^{-2} (geometric area: 0.13 cm^2) was used for preparing all the samples. Specimens of the Pt or Pt/Ru filled alumina membranes for SEM were immersed in 3 mol·L^{-1} NaOH

for 10 min to remove the alumina template, and followed by carefully rinsing with deionized water for several times.

2 Results and Discussion

2.1 Characterization of Nanotubes Array Electrodes

The synthesis of NTAEs using PAA membranes modified with 3-aminopropyltrimethoxysilane was similar to that reported previously[31]. Both the Pt NTAE and PtRu NTAEs with different atomic ratios of Pt to Ru were electrochemically codeposited at -0.1 V from corresponding precursors. From the SEM (Fig. 1A) and TEM images (Fig. 1B), it is clear that Pt and PtRu nanotubles arrays were synthesized. Fig. 1 demonstrates the PtRu NTAE sample with Pt∶Ru =56∶44. The top-view SEM image of the nanotubes array (Fig. 1A) clearly shows the nanotubes array structure of PtRu alloy.

The outer and inner diameters of the nanotubes were (200±20) nm and (60±10) nm, respectively. The thickness of the PtRu nanotubes, which can be controlled by the charge for the codeposition process, is ca. 70 nm in the present case. Interestingly, the TEM image of a single Pt/Ru nanotube (Fig. 1B) shows that the nanotube consists of nanoparticles. The total length of the nanotubes is ca. 3 μm. Electric diffraction pattern shows a polycrystalline Pt/Ru alloy structure (Fig. 1C). XRD measurements of the PtRu nanotubes array (Fig. 1D, curve a) show the characteristics of the face-centered cubic (*fcc*) PtRu crystalline structure with the plane orientations along PtRu (111), PtRu (200), PtRu (220) and PtRu (311). Compared with the diffraction peak position of Pt nanotube array (Fig. 1D, curve b), the reflection peaks of PtRu nanotubes array are shifted to higher 2θ values, demonstrating that the ruthenium atoms in the PtRu alloys fill the platinum lattice sites. This result is similar to that reported previously[33]. The broad bands of the XRD falls demonstrate that the metallic particles in the nanotubes array are small. The average size of the PtRu particles in the nanotubes array is calculated as ca. 11.2 nm from the (111) diffraction peak using the Scherrer's equation[34]. For comparison, the XRD pattern of the pure Pt NTAE is also displayed in Fig. 1D,

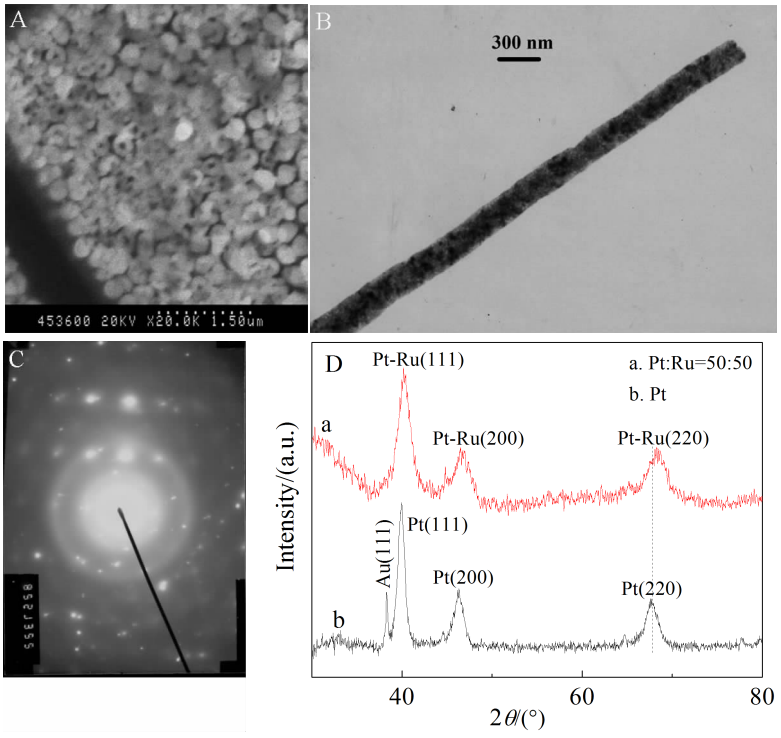

Fig. 1 A. SEM image (top view); B. TEM image; C. ED pattern of the $Pt_{56}Ru_{44}$ nanotubes array codeposited at -0.1 V in silanized PAA template; D. XRD patterns of the $Pt_{56}Ru_{44}$ NTAE (a) and pure Pt NTAE (b)

curve b, which is similar to that of PtRu electrode beside somewhat narrower peaks due to the larger particle size (average particles size: 18.6 nm).

2.2 Determination of the Real Surface Area and Atomic Ratio of the PtRu Electrodes

Comparison of the electrochemical properties of the nanotubes array electrodes can be made by using the real surface area of the NTAEs. For a pure Pt electrode, the area can be determined directly from its voltammogram in a 0.5 mol·L^{-1} H_2SO_4 solution by integrating the charge for the adsorption/desorption of hydrogen as reported previously[35]. In this case, a fractional coverage of 0.77 is taken, and the real surface area is calculated by assuming that a monolayer of adsorbed hydrogen adatoms requires 210 μC·cm^{-2}[30, 36]. However, this approach cannot be directly used to determine the real surface area of PtRu electrode which absorbs hydrogen into the metal lattice[34] due to poorly separated underpotential hydrogen adsorption and overpotential hydrogen evolution regions and undefined double-layer contributions[20].

As known, CO can be adsorbed on both pure Pt-electrode and Ru electrode surfaces to form saturated monolayer [37]. Assuming that each accessible surface Ru atom in the PtRu or Ru nanotubes can adsorb one CO molecule, the real surface area of the NTAEs can then be estimated by the stripping charge of the adsorbed CO (CO_{ad}). Therefore, a full monolayer of CO_{ad} on the PtRu NTAEs was deposited by controlling the adsorption potential at 0.05 V (vs. RHE) in a CO saturated 0.5 mol·L^{-1} H_2SO_4 solution with CO bubbling for 15 min. After adsorption, the dissolved CO in the solution was eliminated by bubbling pure N_2 in the system for another 15 min. Then, a potential step from 0.05 V to 0.71 V was performed to anodically strip the adsorbed CO, and the oxidation current as a function of time was collected simultaneously. A typical result on a $Pt_{60}Ru_{40}$ NTAE is displayed in Fig.2.

The solid curve shows the transient current of the CO adsorbed on the PtRu NTAE. An oxidation current peak having the general characteristics of a surface oxidation process is clearly observed[37]. For

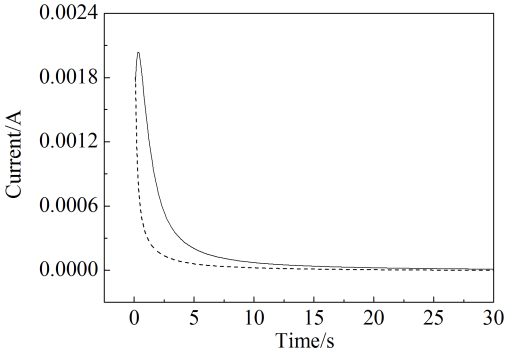

Fig. 2 Current transient of a full monolayer of CO adsorbed on the $Pt_{60}Ru_{40}$ nanotubes array electrode in a solution of 0.5 mol·L^{-1} H_2SO_4 (solid curve). The CO monolayer was formed at 0.05 V from a solution of 0.5 mol·L^{-1} H_2SO_4 saturated with CO and with CO bubbling for 15 min. After the adsorption, the solution was bubbled with nitrogen to remove the dissolved CO in solution. Then a potential step from the CO adsorption potential of 0.05 V to 0.71 V was performed. For subtracting the contribution of the double layer charge, a current transient of the clean NTAE without CO adsorption procedure in 0.5 mol·L^{-1} H_2SO_4 (dashed curve) was collected.

elimina ting the contribution from the double layer charge, a current-time curve of the same electrode in a pure 0.5 mol·L^{-1} H_2SO_4 solution was recorded (Fig. 2, dashed curve). In this case, the transient current decays abruptly to the base signal, and no current maximum is observed during the whole process.Therefore, the coverage of CO_{ad} on the electrode surface can be calculated from the charge under the transient, corrected from the blank experiment (dashed curve). It is assumed that the oxidation of a full monolayer CO which is all top-terminated on the electrode surface generates a charge of 420 μC·cm^{-2}[14, 38]. The real surface area of the PtRu NTAE can then be determined by the following equation.

$$A = \frac{Q(\mu C)}{420(\mu C \cdot cm^{-2})}(cm^2) \quad (1)$$

The bulk compositions (atomic ratios) of the codeposited PtRu NTAEs were directly measured by EDAX. The results are listed in Tab. 1.

It is clear that the atomic ratios of the codeposited PtRu NTAEs deviate from the solution composi-

Tab. 1 The bulk molar compositions (molar ratios) of the electrodeposited electrodes measured by EDAX

Sample	1	2	3	4	5	6	7
Pt(IV):Ru(III)	4:0	3:1	2.7:1.3	2:2	1.3:2.7	1:3	0:4
Pt:Ru	100:0	89:11	60:40	54:46	44:56	19:81	0:100

tions of the metal precursors. This result is somewhat different from that reported previously in which the atomic ratios of the codeposited PtRu alloys on gold electrode were approximately equal to the solution compositions of the metal precursors[38-40]. This difference may be due to the template effect of the PAA membrane modified with molecular anchor of 3-aminopropyltrimethoxysilane.

The electrochemistry of the codeposited PtRu NTAEs with different atomic ratios was first investigated. The CVs of these electrodes in a solution of 0.5 mol·L^{-1} H_2SO_4 at a scan rate of 0.01 V·s^{-1} were recorded and are displayed in Fig. 3.

To avoid the electrochemical dissolution of Ru into solution, potential scan was performed in a potential range of 0.05 to 0.9 V (vs. RHE)[41]. As shown in Fig. 3, the typical features for a polycrystalline Pt and Pt/Ru electrodes can be observed. The currents in the potential range from 0.05 V to 0.40 V are due to the adsorption/desorption of hydrogen adatoms. These currents are directly relating to the Pt content. They increase with the increase of the Pt content in the alloys[42]. The currents in the potential region between 0.40 V and 0.80 V are attributed to the formation and reduction of surface oxygenated species (e.g., OH group) at Ru surface. The shape of the voltammograms correlates, in principle, with the Pt:Ru atomic ratios.

2.3 Activity of the NTAEs Catalysts toward the CO_{ad} Oxidation

In these experiments, CO was adsorbed on the NTAEs at 0.05 V from a CO saturated solution of 0.5 mol·L^{-1} H_2SO_4 with CO bubbling for 15 min. After adsorption, the CO in solution was eliminated by N_2 bubbling through the solution for another 15 min. Then, cyclic voltammograms were recorded anodically from 0.05 V at a scan rate of 0.01 V·s^{-1}. The results for $Pt_{(100-x)}Ru_x$ (x = 0, 11,40, 46, 56, 100) NTAEs

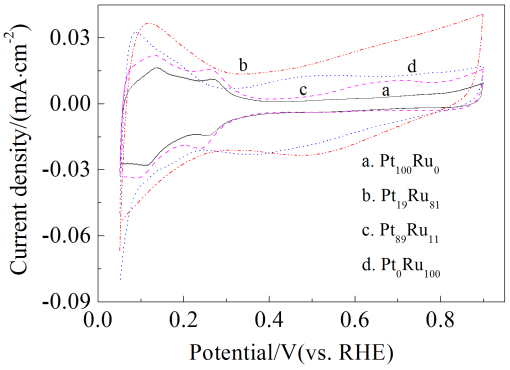

Fig. 3 Cyclic voltammograms (CVs) of a Pt (curve a), $Pt_{19}Ru_{81}$ (curve b), $Pt_{89}Ru_{11}$ (curve c),Pt_0Ru_{100} (curve d) NTAE in a deaerated solution of 0.5 mol·L^{-1} H_2SO_4 at a scan rate of 0.01 V·s^{-1}

are shown in Fig. 4.

The position and shape of the CO oxidation peaks are considerably determined by the Ru content in the PtRu alloys. The CO_{ad} stripping curve on a pure Pt electrode (Fig. 4A) shows a broad current peak centred at approximately 0.70 V with a distinct shoulder at the higher potentials, which is attributed to the contributions from different crystallite orientations[20, 43]. For the PtRu NTAEs, it is evident that small amount of Ru in the alloys promotes the electrocatalytic activity toward the oxidation of CO_{ad} (Fig. 4B-E) as indicated by the negative shift of the onset and peak potentials. For the $Pt_{89}Ru_{11}$ NTAE, the oxidation of CO_{ad} starts at 0.30 V and the current peak appears at 0.58 V. As the atomic ratio of the Ru in the alloys increases from 11% to 46%, the current peak potential shifts slowly from 0.58 V to 0.50 V. With further increase of the atomic ratio of Ru, the current peak potential shifts to more positive potentials again, e.g., the current peak appears at 0.53 V for 56% Ru. It is clear that the PtRu NTAE with 46% Ru is the most active catalyst for the oxidation of CO_{ad}. For a pure Ru electrode (Fig. 4F), the current peak at 0.68 V demonstrates that pure Ru is not a good catalyst for the CO

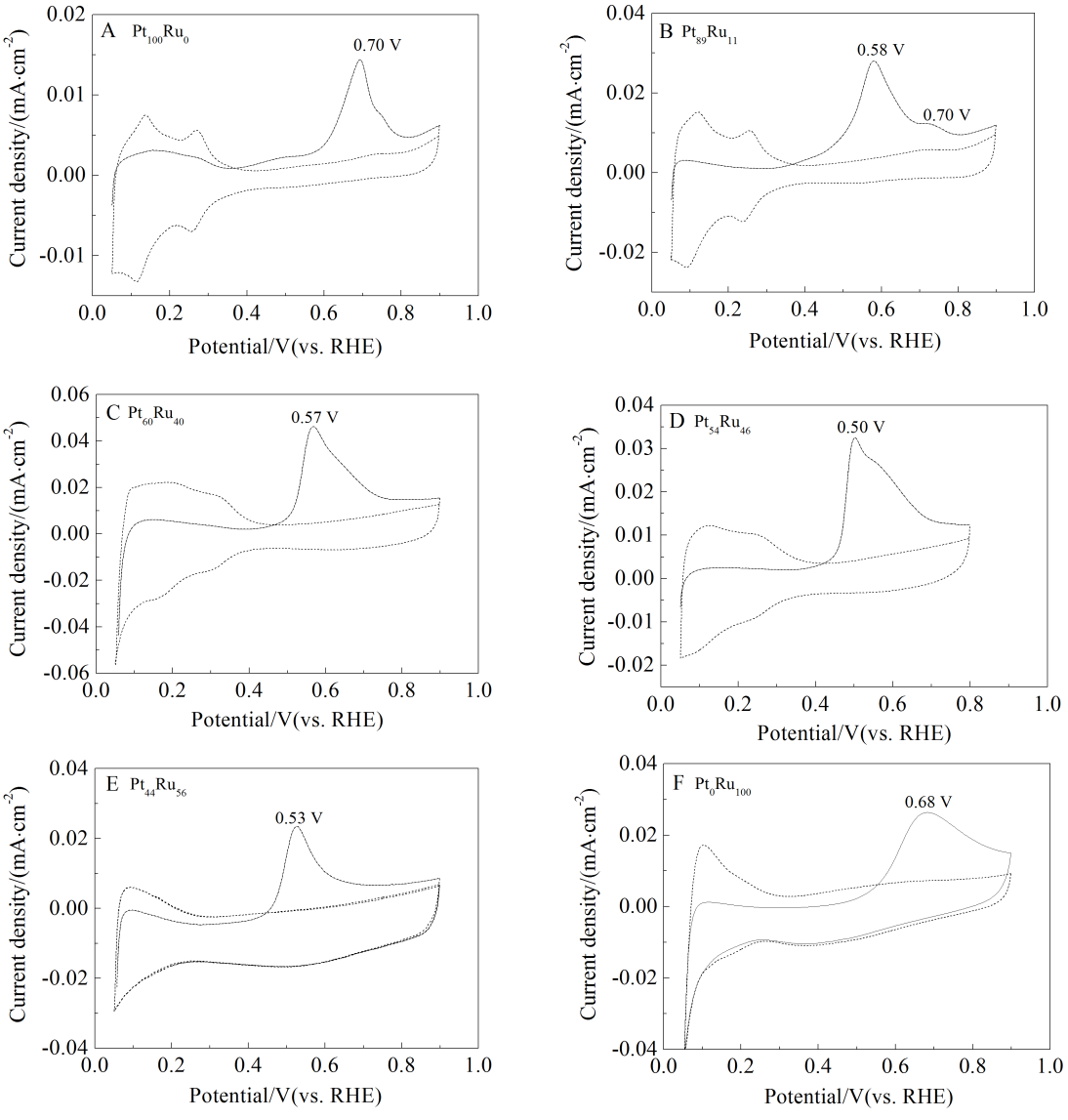

Fig. 4 CVs of a monolayer CO adsorbed on the PtRu NTAEs with different molar ratios in a solution of 0.5 mol·L^{-1} H_2SO_4 (Solid curve) at a scan rate of 0.01 V·s^{-1}. The monolayer of CO on the NTAEs was formed at 0.05 V from a solution of 0.5 mol·L^{-1} H_2SO_4 saturated with CO and with CO bubbling for 15 min. After the adsorption, the solution was bubbled with nitrogen to remove the dissolved CO in solution. Then a cyclic potential sweep was started anodically from this adsorption potential of 0.05 V.

oxidation. The present results for the CO oxidation can be explained by using the bifunctional mechanism [44]. In this study, PtRu NTAE containing ca. 50% Ru has the highest activity for CO electrooxidation, which is in good agreement with the study reported previously[45].

2.4 Activity of the PtRu NTAEs toward Methonal Oxidation

The electrocatalytic activity of the NTAEs toward the electrooxidation of methanol was also investigated. For better understanding the influence of Ru component on the electrocatalytic activity, CVs of the first scan for the PtRu NTAEs in a solution of 0.1 mol·L^{-1} CH_3OH + 0.5 mol·L^{-1} H_2SO_4 at a scan rate of 0.01 V·s^{-1} were recorded. The results on the $Pt_{100-x}Ru_x$ (x = 0, 40, 46, 54, 81, 100) NTAEs are shown in Fig. 5.

Two significant differences are observed for the electrosorption and electrooxidation of methanol on these NTAEs with different Ru content. The electrosorption of methanol on these NTAEs results in

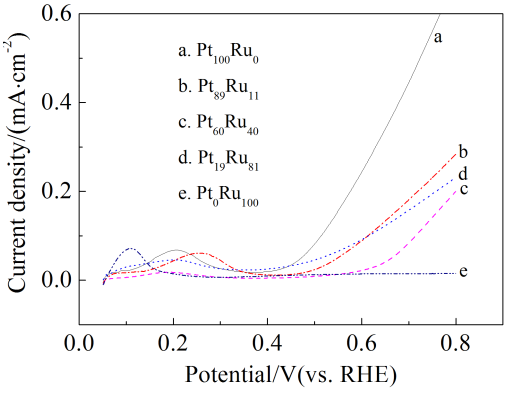

Fig. 5 CVs of the PtRu NTAEs with different molar ratios in a solution of 1 mol·L^{-1} CH_3OH + 0.5 mol·L^{-1} H_2SO_4 at a scan rate of 0.01 V·s^{-1}

the accumulation of poisoning intermediates (e.g., CO_{ad})[14, 37, 44, 46-47] on the electrode surface, blocking further adsorption and direct oxidation of methanol. Therefore, a current peak for this electrosorption occurs. For all the NTAEs containing Ru in the atomic ratio range of 0 to 81, the electrosorption peak islocated at potentials between 0.20 V and 0.3 V. vs RHE. However, for a pure Ru NTAE, the current peak appears at 0.11 V. This peak having almost the same peak potential as the hydrogen desorption peak of the pure Ru NTAE in pure sulfuric acid (Fig. 3) should be due to the desorption of hydrogen, but not the electrosorption of methanol. This is also confirmed by the fact that no current for the oxidation of surface intermediates or direct oxidation of methanol (Fig. 5) appears. This result supports the conclusion that adsorption and oxidation of methanol on pure Ru electrode surface cannot occur[44]. The magnitude of the electrosorption peak current could demonstrate the rate of methanol electrosorption. From Fig. 5, it is clear that the NTAE with 40% Ru ($Pt_{60}Ru_{40}$) has the highest activity toward the electrosorption of methanol (Fig. 5).

Interestingly, the bulk composition of PtRu alloys affects both the kinetics of adsorption and direct oxidation of methanol. In the potential region for hydrogen adsorption and desorption, a current peak around 0.2 V overlapped on the peak of hydrogen adatom desorption occurs, indicating the decomposition of methanol on these samples. The current and potential of this methanol decomposition peak are affected strongly by the Pt to Ru ratio, e.g., for a pure porous Pt electrode, the decomposition current peak of methanol appears at 0.26 V; for the sample with Pt∶Ru = 60∶40, the largest current peak at 0.22 V is observed. The increased current could be due to the fact that the decomposition process of methanol is not a rate-determining step. This result indicates that the content of Ru in the alloys induces the change of electronic properties of the catalysts, which determines the decomposition rate of methanol. However, with the further increase of the Ru molar ratio, the electrosorption peak decreases accordingly due to the poor activity of Ru toward the adsorption of methanol. Pure Pt is known to be the best catalyst for breaking the C—H bond but not for water dissociation, the oxidation of methanol cannot occur below 0.45 V[2, 44]. The strong attenuation of this reaction with increasing Ru content is due to the reduced adsorption activity of methanol on Ru-rich surfaces.

The long-term stability of the nanotubes array PtRu catalysts was investigated in a solution of 0.1 mol·L^{-1} CH_3OH + 0.5 mol·L^{-1} H_2SO_4 at room temperature. As shown in Fig. 6, the steady-state polarization curves of the PtRu electrodes at 0.55 V show that the PtRu catalysts have excellent electrocatalytic activity toward the electrooxidation of methanol and good stability. At polarization time of 500 s, the current density obtained from $Pt_{60}Ru_{40}$ is 0.18 mA·cm^{-2}. In contrast, the current densities obtained from $Pt_{81}Ru_{19}$ and $Pt_{54}Ru_{46}$ catalysts are only ca. 0.02 mA·cm^{-2}. These results demonstrate that $Pt_{60}Ru_{40}$ possesses much stronger anti-poisoning capability than $Pt_{81}Ru_{19}$ and $Pt_{54}Ru_{46}$ catalysts at room temperature.

The above phenomenon can be well understood by taking the bifunctional mechanism into account, in which the Ru sites dissociate water to form surface hydroxides and promote the oxidation of CO on neighboring Pt sites. In good agreement with the results in Fig. 5, the catalyst with Pt∶Ru = 60∶40 shows the highest electrocatalytic activity toward the electrooxidation of methanol at room temperature.

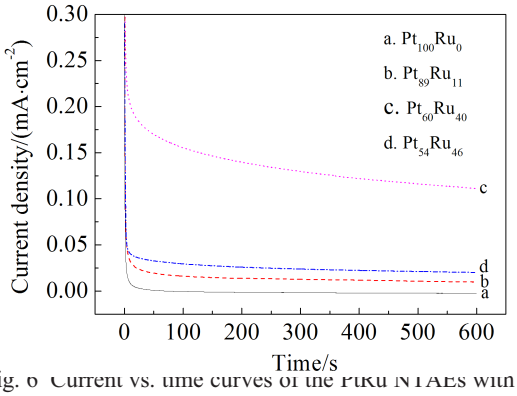

Fig. 6 Current vs. time curves of the PtRu NTAEs with different molar ratios of Pt to Ru at 0.55 V (vs. RHE) in a solution of 1.0 mol·L^{-1} CH_3OH + 0.5 mol·L^{-1} H_2SO_4

3 Conclusion

The bimetallic nanotubes array electrodes (NTAEs) with large surface areas have been prepared by electrochemical codeposition of platinum and ruthenium in a 3-aminopropyltrimethoxysilane modified anodic alumina membranes. The prepared nanoarrays composed of Pt or PtRu alloys (with different molar ratios) could enhance the mass-normalized activity toward the electrooxidation of methanol by improving mass diffusion rate through the catalysts and avoiding the self-aggregation problems that commonly existed for the DMFC anodic electrocatalysts. PtRu NTAE containing ca. 50% Ru has the highest activity for CO electrooxidation and 40% Ru for the CH_3OH electrooxidation at room temperature.

References:

[1] Liu H S, Song C J, Zhang L, et al. A review of anode catalysis in the direct methanol fuel cell[J]. Journal of Power Sources, 2006, 155(2): 95-110.

[2] IwasitaT. Electrocatalysis of methanol oxidation[J]. Electrochimica Acta, 2002, 47(22/23): 3663-3674.

[3] Koczkur K, Yi Q F, Chen A. Nanoporous Pt-Ru networks and their electrocatalytical properties[J]. Advanced Materials, 2007, 19(18): 2648-2652.

[4] Denis M C, Lefevre M, Guay D, et al. Pt-Ru catalysts prepared by high energy ball-milling for PEMFC and DMFC: Influence of the synthesis conditions [J]. Electrochimica Acta, 2008, 53(12): 5142-5154.

[5] Basnayake R, Li Z R, Katar S, et al. PtRu nanoparticle electrocatalyst with bulk alloy properties prepared through a sonochemical method[J]. Langmuir, 2006, 22(25): 10446-10450.

[6] Wakisaka M, Mitsui S, Hirose Y, et al. Electronic structures of Pt-Co and Pt-Ru alloys for CO-tolerant anode catalysts in polymer electrolyte fuel cells studied by EC—XPS[J]. The Journal of Physical Chemistry B, 2006, 110 (46): 23489-23496.

[7] Stamenkovic V, Arenz M, Blizanac B B,et al. *In situ* CO oxidation on well characterized Pt_3Sn (hkl) surfaces: A selective review[J]. Surface Science,2005, 576(1/3): 145-157.

[8] Lim D H, Choi D H, Lee W D, et al. A new synthesis of a highly dispersed and CO tolerant PtSn/C electrocatalyst for low-temperature fuel cell; its electrocatalytic activity and long-term durability[J]. Applied Catalysis B-Environmental, 2009, 89(3/4): 484-493.

[9] Roychowdhury C, Matsumoto F, Zeldovich V B, et al. Synthesis, characterization, and electrocatalytic activity of Pt-Bi and PtPb nanoparticles prepared by borohydride reduction in methanol[J]. Chemistry of Materials, 2006, 18(14): 3365-3372.

[10] Orilall M C, Matsumoto F, Zhou Q, et al. One-pot synthesis of platinum-based nanoparticles incorporated into mesoporous niobium oxide-carbon composites for fuel cell electrodes[J]. Journal of the American Chemical Society, 2009, 131(26): 9389-9395.

[11] Kawaguchi T, Rachi Y, Sugimoto W, et al. Performance of ternary PtRuRh/C electrocatalyst with varying Pt:Ru:Rh ratio for methanol electro-oxidation[J]. Journal of Applied Electrochemistry, 2006, 36(10): 1117-1125.

[12] He C Z, Kunz H R, Fenton J M. Electro-oxidation of hydrogen with carbon monoxide on Pt/Ru-based ternary catalysts[J]. Journal of the Electrochemical Society, 2003,150 (8): A1017-A1024.

[13] Bock C, Blakely M A, Macdougall B. Characteristics of adsorbed CO and CH_3OH oxidation reactions for complex Pt/Ru catalyst systems[J]. Electrochimica Acta, 2005, 50 (12): 2401-2414.

[14] De Souza J P I, Iwasita T, Nart F C, et al. Performance evaluation of porous electrocatalysts via normalization of the active surface[J]. Journal of Applied Electrochemisty, 2000, 30(1): 43-48.

[15] Mickelson L L, Friesen C. Direct observation of bifunctional electrocatalysis during CO oxidation at $Ru_{\theta=0.37}$/Pt {111} surfaces via surface stress measurements [J]. Journal of the American Chemical Society, 2009,131 (41): 14879-14884.

[16] Stamenkovic V R, Arenz M, Lucas C A,et al. Surface chemistry on bimetallic alloy surfaces: Adsorption of anions and oxidation of CO on Pt_3Sn(111)[J]. Journal of the

American Chemical Society, 2003, 125(9): 2736-2745.

[17] Xia X H, Iwasita T. Influence of underpotential deposited lead upon the oxidation of HCOOH in $HClO_4$ at platinumelectrodes[J]. Journal of the Electrochemical Society, 1993,140(9): 2559-2565.

[18] Kijima T, Nagatomo Y, Takemoto H, et al. Synthesis of nanohole-structured single-crystalline platinum nanosheets using surfactant-liquid-crystals and their electrochemical characterization[J]. Advanced Functional Materials, 2009, 19(4): 545-553.

[19] Zhuang L, Jin J, Abruna H D. Direct observation of elec trocatalytic synergy[J]. Journal of the American Chemical Society, 2007, 129(36): 11033-11035.

[20] Jambunathan K, Jayaraman S, Hillier A C. A multielectrode electrochemical and scanning differential electrochemical mass spectrometry study of methanol oxidation on electrodeposited Pt_xRu_y[J].Langmuir, 2004, 20(5): 1856-1863.

[21] Gasteiger H A, Markovic N, Ross P N, et al. Methanol electrooxidation on well-characterized platinum-rutheni um bulk alloys[J]. The Journal of Physical Chemistry, 1993, 97(46): 12020-12029.

[22] Guo Y G, Hu J S, Zhang H M, et al. Tin/platinum bimetallic nanotube array and its electrocatalytic activity for methanol oxidation[J]. Advanced Materials, 2005, 17 (6):746-750.

[23] Song Y Y, Li Y, Xia X H.One-step pyrolysis process to synthesize dispersed Pt/carbon hollow nanospheres catalysts for electrocatalysis[J]. Electrochemistry Communications, 2007, 9(2): 201-205.

[24] Liu Y C, Qiu X P, Huang Y Q, et al. Mesocarbon microbeads supported Pt-Ru catalysts for electrochemical oxidation of methanol[J]. Journal of Power Sources, 2002, 111(1): 160-164.

[25] Martin C R. Nanomaterials: A membrane-based synthetic approach[J]. Science,1994, 266(5193): 1961-1966.

[26] Martin C R. Template synthesis of electronically conductive polymer nanostructures [J]. Ac counts of Chemical Research,1995, 28(2):61-63.

[27] Whitney T M, Jiang J S, Searson P C, et al. Fabrication and magnetic properties of arrays of metallic nanowires [J]. Science, 1993, 261(5126): 1316-1319.

[28] Chen W, Xia X H. An electrokinetic method for rapid synthesis of nanotubes[J]. A European Journal of Chemical Physics and Physical Chemistry,2007, 8(7): 1009-1012.

[29] Keller F, Hunter M S, Robinson D L. Structural features of oxide coatings on aluminum [J].Journal of Electrochemistry Society, 1953,100: 411-419.

[30] Diggle J W, Downie T C, Goulding C W. Anodic oxide films on aluminum[J].Chemical Reviews, 1969, 69(3): 365-405.

[31] Yuan J H, Wang K, Xia X H. Highly ordered platinum nanotubules arrays for amperometric glucose sensing[J]. Advanced Functional Materials, 2005, 15(5): 803-809.

[32] Zhou Y G, Yang S, Qian Q Y,et al. Gold nanoparticles integrated in a nanotube array for electrochemical detection of glucose[J].Electrochemistry Communications, 2009, 11(1):216-219.

[33] Cattaneo C, de Pinto M I S, Mishima H, et al. Characterization of platinum-rutheniumelectrodeposits using XRD, AES and XPS analysis [J].Journal of Electroanalytical Chemistry, 1999, 461(1/2): 32-39.

[34] Cullity B D. Elements of X-ray diffraction [M]. New York: Addison-Wesley Pub. Inc., 1984.

[35] Trasatti S, Petrii O A. Real surface-area measurements inelectrochemistry[J]. Journal of Electroanalytical Chemistry, 1992, 327(1/2):353-376.

[36] Choi J H, Park K W, Park I S, et al. Methanol electro-oxidation and direct methanol fuel cell using Pt/Rh and Pt/Ru/Rhalloy catalysts[J]. Electrochimica Acta, 2004, 50 (2/3): 787-790.

[37] Xia X H, Vielstich W. Enhance oxidation of carbon-monoxide on platinum in $HClO_4$ via interaction with acetonitrile[J]. Electrochimica Acta, 1994, 39(1): 13-21.

[38] Camara G A, de Lima R B, Iwasita T. Catalysis of ethanol electro oxidation by PtRu: The influence of catalyst composition[J]. Electrochemistry Communications, 2004, 6(8): 812-815.

[39] Richarz F, Wohlmann B, Vogel U, et al. Surface and electrochemical characterization of electrodeposited PtRu alloys[J]. Surface Science, 1995, 335(1/3): 361-371.

[40] Zhang X, Chan KY. Water-in-oil microemulsion synthesis of platinum-ruthenium nanoparticles, their characterization and electrocatalytic properties[J]. Chemistry of Materials, 2003, 15(2): 451-459.

[41] Gasteiger H A, Markovic N, Ross P N, et al. Temperature-dependent methanol electrooxidation on well-characterized Pt- Rualloys[J]. Journal of The Electrochemical Society, 1994, 141: 1795-1803.

[42] Hoster H, Iwasita T, Baumgärtner H, et al.Current-time behavior of smooth and porous PtRu surfaces for methanol oxidation[J]. Journal of The Electrochemical Society, 2001, 148(5): A496-A501.

[43] Jusys Z, Kaiser J, Behm R J. Composition and activity of high surface area PtRu catalysts towards adsorbed CO and methanol electrooxidation—A DEMS study[J]. Elec-

trochimica Acta, 2002, 47(22/23): 3693-3706.

[44] Krausa M, Vielstich W. Study of the electrocatalytic influence of Pt/Ru and Ru on the oxida of residues of small organic-molecuels[J]. Journal of Electroanalytical Chemistry, 1994, 379 (1/2): 307-314.

[45] Lin W F, Iwasita T, Vielstich W. Catalysis of CO electrooxidation at Pt, Ru, and PtRu alloy. An *in situ* FTIR study[J]. The Journal of Physical Chemistry B,1999, 103 (16): 3250-3257.

[46] Xia X H, Iwasita T, Ge F, et al. Structural effects and reactivity in methanol oxidation on poly crystalline and single crystal platinum [J].Electrochimica Acta,1996, 41 (5):711-718.

[47] Iwasita T, Xia X H, Liess H D, et al. Electrocatalysis of organic oxidations: Influence of water adsorption on the rate of reaction[J].The Journal of Physical Chemistry B, 1997, 101(38): 7542-7547.

阵列纳米管中铂:钌原子比对甲醇电催化氧化活性的影响

袁金华,王凤彬,夏兴华*

(南京大学 化学化工学院, 生命分析化学国家重点实验室, 江苏 南京 210093)

摘要: 采用电化学沉积技术在 3- 氨丙基三甲基硅氧烷修饰的多孔氧化铝膜板中制备了具有不同 Pt/Ru 原子比的双元 Pt/Ru 阵列纳米管电极 (NTAEs). 分别用 X-射线衍射和扫描电镜表征了催化剂结构和形态. 电化学结果表明,通过控制前驱沉积液的浓度可得到不同 PtRu 原子比的 NTAEs. 所制备的 Pt 或 Pt/Ru 合金阵列纳米电极的真实表面积大、催化活性强,有利于物质传输,对甲醇电氧化显示出较好的催化性能. 实验中还系统研究了催化剂组成与 CO 和 CH_3OH 电催化氧化性能的关系,发现 Pt/Ru = 50:50 的阵列纳米管电极对 CO 电氧化显示出最好的催化活性,而 Ru 原子比为 40%的催化剂对甲醇电氧化呈现最佳催化性能.

关键词: 催化剂;铂钌合金;纳米管;甲醇;一氧化碳